

Chemistry of Unsaturated Group 6 Metal Complexes with Bridging Hydroxy- and Methoxycarbyne Ligands. 2. Synthesis, Structure, and Bonding of 32- and 34-Electron Complexes[§]

M. Esther García,[†] Daniel García-Vivó,[†] Miguel A. Ruiz,^{*,†} Santiago Alvarez,[‡] and Gabriel Aullón[‡]

Departamento de Química Orgánica e Inorgánica/IUQOEM, Universidad de Oviedo, E-33071 Oviedo, Spain, and Departamento de Química Inorgánica, Universidad de Barcelona, E-08028 Barcelona, Spain

Received July 20, 2007

The reaction of the 30-electron methoxycarbyne complex $[\text{Mo}_2\text{Cp}_2(\mu\text{-COMe})(\mu\text{-PCy}_2)(\mu\text{-CO})]$ with carbon monoxide gives quantitatively the electron-precise derivative $[\text{Mo}_2\text{Cp}_2(\mu\text{-COMe})(\mu\text{-PCy}_2)(\text{CO})_3]$, in which the methoxycarbyne ligand adopts a highly asymmetric semibridging coordination mode. This tricarbonyl species dissociates one of its CO ligands under thermal conditions (333 K) to give the 32-electron complex $[\text{Mo}_2\text{Cp}_2(\mu\text{-COMe})(\mu\text{-PCy}_2)(\text{CO})_2]$ in high yield. The structures and bonding of both complexes, as well as that of the isostructural carboxycarbyne complex $[\text{Mo}_2\text{Cp}_2\{\mu\text{-C}(\text{CO}_2\text{Me})\}(\mu\text{-PCy}_2)(\text{CO})_2]$ were studied by means of density functional theory. These calculations allow us to describe the intermetallic interaction in the edge-sharing bioctahedral dicarbonyls by a configuration of the type $\delta^2\sigma^2\pi^2(\delta^*)^2$, with the δ^* orbitals being involved in π back-bonding to the carbonyl ligands, and the δ orbitals significantly delocalized over the $\text{Mo}_2\text{C}(\text{carbyne})$ triangle, then becoming the π -bonding component of the metal–carbyne bond. For these complexes, an atoms-in-molecules (AIM) analysis allows us to locate the corresponding intermetallic bond critical points, these exhibiting relatively high values of the electron density (ca. $0.43 \text{ e } \text{\AA}^{-3}$). Both the MO and AIM analysis of these dicarbonyl complexes suggest that the binding of the methoxy- and carboxycarbyne ligands to the dimetal center is quite similar.

Introduction

In the previous part of this series we have shown that a variety of cationic hydroxy- and methoxycarbyne complexes of the type $[\text{M}_2\text{Cp}_2(\mu\text{-COR})(\mu\text{-PR}'_2)_2]\text{BF}_4$ ($\text{M} = \text{W}$, $\text{R} = \text{Me}$, $\text{R}' = \text{Ph}$; $\text{M} = \text{Mo}$, $\text{R} = \text{H}$, Me , $\text{R}' = \text{Et}$) and $[\text{Mo}_2\text{Cp}_2(\mu\text{-COR})(\mu\text{-COR}')(\mu\text{-PCy}_2)]\text{BF}_4$ ($\text{R} = \text{R}' = \text{Me}$; $\text{R} = \text{Me}$, $\text{R}' = \text{H}$, Et) can be easily obtained by the reaction of the corresponding neutral monocarbonyl precursors with either $\text{HBF}_4 \cdot \text{OEt}_2$ or $[\text{Me}_3\text{O}]\text{BF}_4$.¹ We also reported there a complete theoretical study of these systems, proving the usefulness of density functional theory (DFT)² methods for the interpretation of the electronic structure and bonding in these highly unsaturated binuclear complexes. Indeed, the use of the hybrid functional B3LYP for these face-sharing bioctahedral complexes not only leads to an excellent agreement between optimized and experimentally determined geometries, but also allow us to describe the intermetallic bond as one of order three following from the configuration $\sigma^2\delta^4$. We should note, however, that in these complexes the δ -bonding orbitals are delocalized over the $\text{Mo}_2\text{C}(\text{carbyne})$ triangle and hence constitute the π -bonding component of the metal–carbyne interaction. Therefore, a reduction of the direct overlap between the metal atoms occurs as a consequence of the formation of the metal–carbon multiple bond of the alkoxy-carbyne ligand,

which in turn retains some multiplicity in its C–O bond (originally a double bond in the corresponding carbonyl-bridged precursor).

We have noted previously that the study of the reactivity of hydroxy- and alkoxy-carbyne ligands at unsaturated binuclear centers might be of interest not only because of the unusual transformations that can be induced,³ but also in the context of important academic and industrial reactions like the metal-catalyzed hydrogenation of CO.⁴ We thus initiated a systematic study of the reactivity of the above-mentioned 30-electron hydroxy- and alkoxy-carbyne complexes, the results of which will be reported separately. Besides, to expand the range of reactive substrates at hand, we were also interested in preparing related alkoxy-carbyne complexes with metal–metal bond orders lower than three, so we could examine the effect of these weaker intermetallic interactions upon the metal–carbyne binding and the reactivity associated with it. In this paper we report full details of our study of the 32- and 34-electron complexes derived from the addition of one or two CO ligands to the 30-electron complex $[\text{Mo}_2\text{Cp}_2(\mu\text{-COMe})(\mu\text{-PCy}_2)(\mu\text{-CO})]$ (**1**).⁵ To better understand the effects of the added ligands upon the metal–metal and metal–carbyne bonding we have analyzed the

* To whom correspondence should be addressed. E-mail: mara@uniovi.es.

[§] This paper is dedicated to the memory of Dr. Lorenzo Pueyo, distinguished professor of physical chemistry at the Universidad de Oviedo.

[†] Universidad de Oviedo.

[‡] Universidad de Barcelona.

(1) García, M. E.; García-Vivó, D.; Ruiz, M. A.; Alvarez, S.; Aullón, G. *Organometallics* **2007**, *26*, 4930.

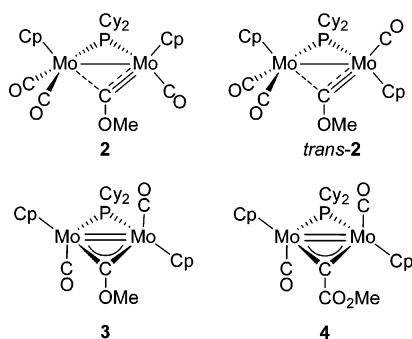
(2) (a) Koch, W.; Holthausen, M. C. *A Chemist's Guide to Density Functional Theory*, 2nd ed.; Wiley-VCH: Weinheim, Germany, 2002. (b) Ziegler, T. *Chem. Rev.* **1991**, *91*, 651.

(3) (a) Alvarez, C. M.; Alvarez, M. A.; García, M. E.; García-Vivó, D.; Ruiz, M. A. *Organometallics* **2005**, *24*, 4122. (b) Alvarez, M. A.; García, M. E.; Riera, V.; Ruiz, M. A.; Robert, F. *Organometallics* **2002**, *21*, 1177. (c) Alvarez, M. A.; García, M. E.; Riera, V.; Ruiz, M. A. *Organometallics* **1999**, *18*, 634. (d) Alvarez, M. A.; Bois, C.; García, M. E.; Riera, V.; Ruiz, M. A. *Angew. Chem., Int. Ed. Engl.* **1996**, *35*, 102. (e) García, M. E.; Riera, V.; Rueda, M. T.; Ruiz, M. A.; Halut, S. *J. Am. Chem. Soc.* **1999**, *121*, 1960.

(4) (a) Maitlis, P. M. *J. Mol. Catal. A* **2003**, *204–205*, 55. (b) Campbell, I. M. *Catalysis at Surfaces*; Chapman and Hall: New York, 1988.

(5) García, M. E.; Melón, S.; Ramos, A.; Riera, V.; Ruiz, M. A.; Belletti D.; Graiff, C.; Tiripicchio, A. *Organometallics* **2003**, *22*, 1983.

Chart 1



structure and bonding within the new alkoxy-carbyne complexes using DFT methods and subsequent MO and AIM analysis, following the scheme used previously with the 30-electron alkoxy-carbyne complexes.¹ A parallel study of the carboxy-carbyne complex $[\text{Mo}_2\text{Cp}_2\{\mu\text{-C}(\text{CO}_2\text{Me})\}(\mu\text{-PCy}_2)(\text{CO})_2]$ also has been performed, this allowing us to compare the metal-carbon binding of the methoxycarbonyne ligand with that of a non-alkoxy carbyne ligand. With the current study we thus complete a wide analysis of the structure and bonding of alkoxy-carbyne-bridged complexes of the group 6 elements having intermetallic bond orders ranging formally from 3 to 1.

Results and Discussion

Reaction of Compound 1 with Carbon Monoxide. Organometallic compounds having unsaturated dimetal centers are usually reactive toward carbon monoxide,⁶ to give the corresponding addition products. Thus, it is not surprising that compound **1** reacts with CO when its solutions are stirred overnight under a slight overpressure (p_{CO} ca. 4 atm) to give the electron-precise tricarbonyl derivative $[\text{Mo}_2\text{Cp}_2(\mu\text{-COMe})(\mu\text{-PCy}_2)(\text{CO})_3]$ (**2**) in quantitative yield (Chart 1), although no intermediates are detected in this somewhat slow process. The tricarbonylic nature of compound **2** is clearly denoted by the presence of three strong C–O stretching bands in its IR spectrum (Table 1). The frequencies and intensities of these bands are very similar to those found for the isoelectronic complexes $[\text{Mo}_2\text{Cp}_2(\mu\text{-PEt}_2)_2(\text{CO})_3]$ ⁷ and $[\text{Mo}_2(\mu\text{-}\eta^5\text{-C}_5\text{H}_4\text{-SiMe}_2\text{C}_5\text{H}_4)(\mu\text{-PMe}_2)_2(\text{CO})_3]$,⁸ in which the three carbonyl ligands are placed on the same side of the average plane defined by the metal and phosphorus atoms, as confirmed for the latter compound through an X-ray study. Therefore, a similar cisoid geometry is assumed for compound **2**. Moreover, we have shown in the previous part of this series that the DFT-calculated frequencies and intensities for the C–O stretches of the carbonyl and methoxycarbonyne ligands in our complexes are in good agreement with the experimental values measured by IR spectroscopy.¹ Therefore we can confidently use calculated values of intensity and frequency to distinguish between different isomeric structures. In particular, as we will discuss later in the context of the DFT calculations of compound **2**, the interaction between the $\text{M}(\text{CO})$ and $\text{M}(\text{CO})_2$ oscillators in this molecule is strong enough to give rise to two substantially different patterns

of the C–O stretches depending on the relative arrangement of the $\text{CpMo}(\text{CO})_x$ fragments (cis or trans with respect to the average Mo_2PC plane; see Chart 1). As can be appreciated in the Figure 2, the experimental pattern of the IR spectrum of compound **2** in the C–O stretching region is in excellent agreement with that calculated for the cisoid structure, and it is significantly different from that calculated for *trans*-**2**, thus excluding the presence of significant amounts of the latter isomer in the solutions of this compound. In agreement with such an asymmetric structure, the CO ligands of **2** give rise to three ¹³C NMR resonances in the terminal region, whereas the Cp ligands exhibit two distinct chemical environments. Unexpectedly, the bridging carbyne atom displays a relatively low chemical shift (300.7 ppm), when compared to those found for our previous 30-electron alkoxy- or hydroxycarbonyne complexes (ca. 365 ppm),¹ or other alkoxy-carbyne-bridged complexes described in the literature.^{3,5,9} This feature can be mainly attributed to the highly asymmetric coordination of the alkoxy-carbyne ligand in **2**, as predicted by the DFT calculations (see later), yielding Mo–C(carbyne) distances differing by ca. 0.45 Å (Table 2), with the short distance approaching the value found in the only terminal methoxycarbonyne complex reported so far, $[\text{WTP}'(\text{COMe})(\text{CO})_2]$ ($\text{Tp}' = \text{HB}(\text{N}_2\text{C}_3\text{Me}_2\text{H})_3$),¹⁰ which is also characterized by a quite shielded carbyne resonance (δ_{C} 228.2 ppm). As for the phosphide bridge, we note that it gives rise to a ³¹P NMR resonance with a chemical shift (219.7 ppm) similar to those measured for other electron-precise dimolybdenum phosphide-bridged complexes such as the tricarbonyl $[\text{Mo}_2\text{Cp}_2(\mu\text{-PEt}_2)_2(\text{CO})_3]$ (194.7 ppm) or the hydride-phosphide complex $[\text{Mo}_2\text{Cp}_2(\mu\text{-H})(\mu\text{-PCy}_2)(\text{CO})_4]$ (218.8 ppm).⁷

Decarbonylation Reaction of Compound 2. Tricarbonyl complexes of the group 6 elements such as **2** are rare species, placed midway between the usually more stable tetracarbonylic or dicarbonylic structures ($[\text{M}_2\text{Cp}_2(\mu\text{-X})(\mu\text{-Y})(\text{CO})_n]$, $n = 2, 4$). For instance, the related complex $[\text{Mo}_2\text{Cp}_2(\mu\text{-PEt}_2)_2(\text{CO})_3]$ experiences a spontaneous decarbonylation at room temperature to give the *trans*-dicarbonyl complex *trans*- $[\text{Mo}_2\text{Cp}_2(\mu\text{-PEt}_2)_2(\text{CO})_2]$ in high yield.⁷ Thus, we decided to study the decarbonylation reactions of **2** as a potential route to the corresponding unsaturated dicarbonyl complex. Photolysis of a toluene solution of compound **2** with visible-UV light induces rapidly a double decarbonylation process whereby compound **1** is rapidly and cleanly regenerated, with no intermediates being detected. However, when toluene solutions of **2** are heated at 333 K, a single decarbonylation occurs progressively (45 min) to give the *trans*-dicarbonyl complex $[\text{Mo}_2\text{Cp}_2(\mu\text{-COMe})(\mu\text{-PCy}_2)(\text{CO})_2]$ (**3**) in high yields (Chart 1). The process is reversible, so the tricarbonyl **2** can be regenerated in ca. 6 h at room temperature by stirring a toluene solution of **3** under a slight CO overpressure (p_{CO} ca. 4 atm). Finally, we should point out that no further decarbonylation can be induced thermally.

(6) (a) Collman, J. P.; Boulatov, R. *Angew. Chem., Int. Ed.* **2002**, *41*, 3948. (b) Winter, M. J. *Adv. Organomet. Chem.* **1989**, *29*, 101. (c) Curtis, M. D. *Polyhedron* **1987**, *6*, 759. (d) Cotton, F. A.; Walton, R. A. *Multiple Bonds Between Metal Atoms*, 2nd ed.; Oxford University Press: Oxford, UK, 1993.

(7) García, M. E.; Riera, V.; Ruiz, M. A.; Rueda, M. T.; Sáez, D. *Organometallics* **2002**, *21*, 5515.

(8) (a) Heck, J. *J. Organomet. Chem.* **1986**, *311*, C5. (b) Abriell, W.; Baum, G.; Burdof, H.; Heck, J. *Z. Naturforsch.* **1991**, *46b*, 841.

(9) (a) Hersh, W. H.; Fong, R. H. *Organometallics* **2005**, *24*, 4179. (b) Peters, J. C.; Odon, A. L.; Cummins, C. C. *Chem. Commun.* **1997**, 1995. (c) Bronk, B. S.; Protasiewicz, J. D.; Pence, L. E.; Lippard, S. J. *Organometallics* **1995**, *14*, 2177. (d) Seyferth, D.; Ruschke, D. P.; Davis, W. H. *Organometallics* **1994**, *13*, 4695. (e) Chi, Y.; Chuang, S. H.; Chen, B.-F.; Peng, S.-M.; Lee, G.-H. *J. Chem. Soc., Dalton Trans.* **1990**, 3033. (f) Friedman, A. E.; Ford, P. C. *J. Am. Chem. Soc.* **1989**, *111*, 551. (g) Keister, J. B. *Polyhedron* **1988**, *7*, 847. (h) Friedman, A. E.; Ford, P. C. *J. Am. Chem. Soc.* **1986**, *108*, 7851. (i) Farrugia, L. J.; Miles, A. D.; Stone, F. G. A. *J. Chem. Soc., Dalton Trans.* **1985**, 2437. (j) Beanan, L. R.; Keister, J. B. *Organometallics* **1985**, *4*, 1713. (k) Nuel, D.; Dahan, F.; Mathieu, R. *J. Am. Chem. Soc.* **1985**, *107*, 1658. (l) Shapley, J. R.; Yeh, W.-Y.; Churchill, M. R.; Li, Y.-J. *Organometallics* **1985**, *4*, 1898. (m) Green, M.; Mead, K. A.; Mills, R. M.; Salter, I. D.; Stone, F. G. A.; Woodward, P. *J. Chem. Soc., Chem. Commun.* **1982**, 51.

(10) Stone, K. C.; White, P. S.; Templeton, J. L. *J. Organomet. Chem.* **2003**, *684*, 13.

Table 1. Selected IR^a and NMR^b Data for Compounds 1–4

compd	$\nu(\text{CO})$	$\delta(\text{P})$	$\delta(\mu\text{-C}) [J_{\text{CP}}]$
[Mo ₂ Cp ₂ (μ -COMe)(μ -PCy ₂)(μ -CO)] (1) ^c	1672 (s)	227.8	352.0 [15] ^d
[Mo ₂ Cp ₂ (μ -COMe)(μ -PCy ₂)(CO) ₃] (2)	1933 (vs), 1860 (s), 1843 (m, sh)	219.7	300.7 [9]
[Mo ₂ Cp ₂ (μ -COMe)(μ -PCy ₂)(CO) ₂] (3)	1894 (w, sh), 1863 (s)	125.0	404.0 [5]
[Mo ₂ Cp ₂ { μ -C(CO ₂ Me)}(μ -PCy ₂)(CO) ₂] (4) ^e	1929 (w, sh), 1900 (vs)	128.2 ^f	402.8 ^f

^a Recorded in dichloromethane solution, ν in cm⁻¹. ^b Recorded in CD₂Cl₂ solutions at 290 K and 121.50 (³¹P) or 75.48 (¹³C) MHz, unless otherwise stated; δ in ppm relative to internal TMS (¹³C) or external 85% aqueous H₃PO₄ (³¹P); J in Hz. ^c Data taken from ref 5. ^d COME ligand. ^e Data taken from ref 3a. ^f In benzene-*d*₆ solutions.

Table 2. Selected DFT-Optimized Bond Lengths (Å) and Angles (deg)^a

parameter	2	<i>trans</i> - 2	3	4 ^b
Mo1–Mo2	3.158	3.176	2.734	2.699 {2.656(1)}
Mo1–C*	2.343	2.357	2.015	2.000 {1.993(5)}
Mo2–C*	1.902	1.902	2.027	2.006 {1.977(6)}
Mo1–CO	1.967	1.985	1.970	1.981 {1.993(8)}
	1.981	1.975		
Mo2–CO	1.954	1.948	1.973	1.978 {2.015(7)}
C*–O	1.316	1.315	1.321	
C*–CO ₂ Me				1.455 {1.447(8)}
O–Me	1.447	1.449	1.440	1.430 {1.448(7)}
C=O				1.220 {1.215(7)}
C(O)–OMe				1.364 {1.353(7)}
Mo1–P	2.613	2.621	2.449	2.454 {2.409(2)}
Mo2–P	2.414	2.421	2.463	2.460 {2.394(2)}
C–O–Me	117.3	116.7	119.3	
Mo2–C–O	149.3	150.6	143.8	138.1 ^c

^a Mo1 refers to the atom positioned *trans* to the methyl group of the COME ligand, except for compound **4**, for which the labeling is arbitrary; C* refers to the bridgehead atom of the carbyne ligand. ^b Experimental values for **4** given in braces (see ref 11). ^c Mo2–C–C angle.

Indeed, when toluene solutions of **2** were heated at temperatures higher than 333 K just a generalized decomposition took place to give a complex mixture of products, none of them being the monocarbonyl complex **1**.

The structural characterization of compound **3** can be made easily by comparison of its spectroscopic data (Table 1) with those previously reported for the related bis(phosphide) complexes [M₂Cp₂(μ -PR₂)₂(CO)₂],⁷ and with those of the carboxy-carbyne complex [Mo₂Cp₂{ μ -C(CO₂Me)}(μ -PCy₂)(CO)₂] (**4**) (Chart 1). The latter was recently prepared by us upon demethylation of the dimethoxyacetylene complex [Mo₂Cp₂{ μ - η^2 : η^2 -C₂(OMe)₂}(μ -PCy₂)(CO)₂]BF₄,^{3a} and its structure has been confirmed through an X-ray study.¹¹ The IR spectrum of **3** shows two C–O stretching bands with the typical pattern of *trans*-dicarbonyl complexes defining angles between the CO ligands close to 180° (weak and strong, in order of decreasing frequencies),¹² while its ³¹P NMR spectrum exhibits a resonance at 125.0 ppm, in the range found for other related 32-electron compounds of type *trans*-[Mo₂Cp₂(μ -PCy₂)(μ -X)(CO)₂] (X = 3e-donor ligand),^{3a,5,7} all of them formally displaying a Mo=Mo double bond. The bridging methoxycarbyne ligand gives rise to a highly deshielded ¹³C NMR resonance at 404.0 ppm, a chemical shift similar to that found for the complex **4** (402.8 ppm). We note that these values are some 30–50 ppm higher than those reported for other complexes displaying bridging alkoxy-carbyne ligands,^{1,3,5,9} this deshielding effect probably being related to the large magnetic anisotropy of the multiple metal–metal bonds.^{6b} Finally, compound **3** was found to exhibit dynamic behavior in solution, as concluded from the presence in the ¹H and ¹³C NMR spectra of just one resonance for both

cyclopentadienyl rings, which are inequivalent in the static structure (Chart 1). This fluxional behavior can be attributed to the rotation, fast on the NMR time scale, of the OMe group around the O–C(carbyne) bond and it has been studied in detail previously for other alkoxy-carbyne complexes,^{1,3c,13} therefore this was not further investigated.

Computational Studies. As we have shown in the previous part of this series, the use of DFT methods for our 30-electron methoxycarbyne-bridged complexes leads to optimized geometries in excellent agreement with those experimentally determined through X-ray diffraction studies. Moreover, the analysis of the Kohn–Sham (KS) molecular orbitals has been shown to be a valuable tool to gain insight into the metal–metal and metal–carbon bonding in these highly unsaturated systems.

With this in mind, we have carried out similar DFT calculations (see the Experimental Section for further details) for the new methoxycarbyne complexes **2** (for both the *cis*- and *trans*-isomers) and **3**, and for the carboxy-carbyne complex **4**. The latter two complexes are isoelectronic and isostructural, both of them exhibiting an edge-sharing bioctahedral geometry, and provide an excellent opportunity to analyze the differences in the bonding between an alkoxy-carbyne ligand and the better known alkylidyne ligands, the latter lacking the possibility of any partial π C–O interaction. In addition, the results of these calculations will allow us to examine the influence of the intermetallic interaction (with formal bond orders of one and two for the tricarbonyl and dicarbonyl species, respectively) on the metal–alkoxy-carbyne binding. Following the scheme used in our previous work,¹ we will first discuss the optimized geometries for these molecules, this being followed by an analysis of the electronic structure and bonding in these complexes from two different points of view, the properties of the relevant molecular orbitals, and the topological properties of the electron density as managed in the AIM theory.¹⁴

Optimized Geometry of the Dicarbonyl Complexes 3 and 4. The most relevant parameters derived from the geometry optimization of the dicarbonyls **3** and **4**, and for the two isomers of the tricarbonyl **2** can be found in Table 2, with the corresponding views being collected in Figure 1. The experimental data from the X-ray diffraction of compound **4** are also collected in Table 2 for comparative purposes.¹¹ As can be seen for this latter complex, the optimized bond lengths are in quite good agreement with the corresponding experimental data, although those involving the metal atoms tend to be slightly longer (less than 0.05 Å) than the corresponding values

(13) For examples of fluxional behavior, see for example: (a) Bavaro, L. M.; Keister, J. B. *J. Organomet. Chem.* **1985**, 287, 357. (b) Keister, J. B.; Payne, M. W.; Muscatella, M. J. *Organometallics* **1983**, 2, 219. (c) Johnson, B. F. G.; Lewis, J.; Orpen, A. G.; Raithby, P. R.; Süß, G. *J. Organomet. Chem.* **1979**, 173, 187. (d) Keister, J. B. *J. Chem. Soc., Chem. Commun.* **1979**, 214. (e) Gavens, P. D.; Mays, M. J. *J. Organomet. Chem.* **1978**, 162, 389.

(14) (a) Bader, R. F. W. *Atoms in Molecules—A Quantum Theory*; Oxford University Press: Oxford, UK, 1990. (b) Bader, R. F. W. *Chem. Rev.* **1991**, 91, 893.

(11) García, M. E.; García-Vivó, D.; Ruiz, M. A. Unpublished results.

(12) Braterman, P. S. *Metal Carbonyl Spectra*; Academic Press: London, UK, 1975.

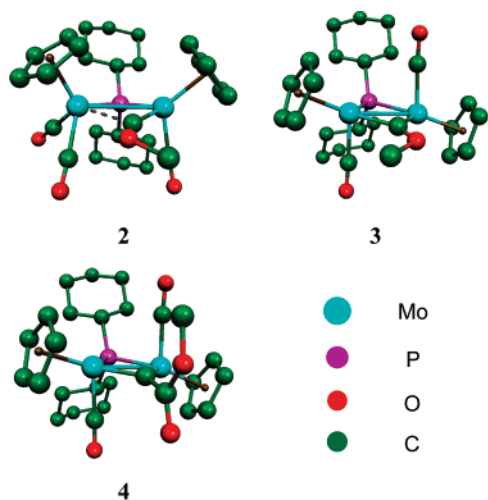


Figure 1. Optimized geometries for complexes **2**, **3**, and **4**, with hydrogen atoms omitted for clarity.

measured in the solid state. We also found this tendency for our 30-electron face-sharing bioctahedral complexes bearing bridging methoxycarbonyl ligands,¹ and this is in any case a common finding with the functionals currently used in the DFT computations of transition-metal complexes.^{6b,2a,15}

The intermetallic distances calculated for the dicarbonyls **3** and **4** (ca. 2.70 Å) are in good agreement with the double metal–metal bond that is to be proposed for these 32-electron complexes according to EAN formalism. As expected, these values are significantly longer (ca. 0.2 Å) than those previously calculated for our triply bonded face-sharing bioctahedral complexes,¹ doubtless as a consequence both of the decrease in the metal–metal bond order (from 3 to 2) as well as in the number of bridging ligands (also from 3 to 2). The geometrical parameters are quite similar for both complexes, although the interatomic distances within the Mo₂C triangle are longer for **3**, by ca. 0.03 (Mo–Mo) and 0.02 Å (Mo–C bonds). There are two factors that could explain these observations. First, there might be a genuine steric effect derived from the presence of the methoxyl group in the same plane containing the metal and carbonyl atoms in the first compound. Second, a slight lengthening of the Mo–C bonds might also be expected if some π_{C-O} interaction in the methoxycarbonyl ligand were to be present, which is detrimental to the π_{M-C} bonding interaction, as found previously for our 30-electron methoxycarbonyl complexes.¹ A related competing interaction is not possible for the carboxycarbonyl complex **4**, hence its shorter Mo–C lengths. In line with this, the calculated distance for the C–C(carbonyl) bond in **4** is 1.46 Å, a value typical for single bonds between sp²-hybridized C atoms,¹⁶ while the value of 1.32 Å for the corresponding C–O bond in **3** is somewhat shorter than those found for comparable single bonds, such as the C(sp²)–O bonds in organic molecules (ca. 1.35 Å),^{16b} or that found for the ester moiety of the carboxycarbonyl ligand of **4** (1.36 Å). This can be taken as indicative of the presence of some multiplicity in this bond, which is consistent with the conformation of the COMe ligand (arrangement in the Mo₂C plane, with the

Table 3. Calculated and Experimental C–O Stretching Frequencies^a

compd	$\nu(C-O)/\text{cm}^{-1}$		percent ^d
	calcd ^b	exp ^c	
2	2037 (100)	1947 (vs)	4.6
	1981 (55)	1882 (s)	5.2
	1971 (56)	1870 (s)	5.4
	1319 (37)		
<i>trans</i> - 2	2033 (77)		
	1976 (53)		
	1954 (100)		
	1318 (43)		
3	1990 (20)	1894 (sh, w)	5.1
	1976 (100)	1862 (vs)	6.1
	1296 (20)		
4	2018 (28)	1929 (sh, w)	4.6
	1992 (100)	1900 (vs)	4.8
	1750 (21)	1652 (w, C=O)	5.9

^a Values corresponding to the CO, CCO₂Me, or COMe ligands, with relative intensities in parentheses; experimental data for **4** taken from ref 3a. ^b Uncorrected values. ^c In petroleum ether (**2**) or CH₂Cl₂ solutions (**3**, **4**). ^d (calcd – exp)/exp.

C–O–C angle close to 120°), and is also in agreement with the MO and AIM analysis to be discussed later on.

A frequency analysis for the dicarbonyls **3** and **4** ensured that the optimized geometries correspond to real minima of the potential energy surface (PES), since no imaginary frequencies were found. The calculated and experimental values of the C–O stretching frequencies for both the carbonyl and the methoxycarbonyl ligands for the dicarbonyls **3** and **4** are shown in Table 3. The calculated values overestimate the experimental figures by ca. 5–6%, which seems to be a normal bias for DFT-derived IR stretching frequencies.^{1,17} For the neutral complex **1**, the C–O stretching frequency of the methoxycarbonyl ligand was calculated previously to be 1315 cm⁻¹, and this relatively high value was taken as another piece of evidence for the persistence of some π_{C-O} interaction within the methoxycarbonyl ligand, also in agreement with the subsequent MO and AIM analysis.¹ In the case of **3**, the calculated C–O stretching frequency (1296 cm⁻¹) is comparable to the above figure, and therefore similar conclusions can be extracted.

The electronic charges computed for these dicarbonyl molecules have been collected in Table S1 (see the Supporting Information), which includes Mulliken charges¹⁸ as well as those derived from the NBO analysis (NPA charges).¹⁹ For both complexes, the highest negative atomic charges are found at the oxygen atoms of the carbonyl ligands, in agreement with their great π -acidity and the large electronegativity of the oxygen atoms. As expected, the atomic charge at the C(carbonyl) atoms is highly dependent on the group directly attached to it. The carboxycarbonyl complex **4** displays a high negative charge of –0.39 (Mulliken) or –0.24 e (NPA) at this site, in good agreement with the figures previously calculated for model compounds with terminal carbonyl ligands such as [CrCl(CH)(CO)₄] (–0.42 e) and [Cr(CH)(CO)₅]⁺ (–0.32 e).²⁰ However,

(17) Yu, L.; Srinivas, G. N.; Schwartz, M. *J. Mol. Struct. (THEOCHEM)* **2003**, 625, 215.

(18) Mulliken, R. S. *J. Chem. Phys.* **1955**, 23, 1833.

(19) Mulliken population analyses fail to give a useful and reliable characterization of the charge distribution in many cases, especially when highly ionic compounds and diffuse basis functions are involved. Charges calculated according to the Natural Population Analysis (NPA) do not show these deficiencies and are more independent of the basis set: (a) Reed, A. E.; Weinstock, R. B.; Weinhold, F. *J. Chem. Phys.* **1985**, 83, 735. (b) Reed, A. E.; Curtis, L. A.; Weinhold, F. *Chem. Rev.* **1988**, 88, 899.

(20) Ushio, J.; Nakatsuji, H.; Yonezawa, T. *J. Am. Chem. Soc.* **1984**, 106, 5892.

(15) Cramer, C. J. *Essentials of Computational Chemistry*, 2nd ed.; Wiley: Chichester, UK, 2004.

(16) (a) Huheey, J. E.; Keiter, E. A.; Keiter, R. L. *Inorganic Chemistry: Principles of Structure and Reactivity*, 4th ed.; HarperCollins College Publishers: New York, 1993. (b) Allen, F. H.; Kennard, O.; Watson, D. G.; Brammer, L.; Orpen, G.; Taylor, R. *J. Chem. Soc., Perkin Trans. 2* **1987**, S1.

for complex **3**, with a methoxyl substituent at the carbyne ligand, we found a significantly lower electron density at the C(carbyne) atom, which turns out to be almost negligible (-0.03 e, Mulliken) or slightly positive ($+0.21$, NPA), with values quite similar to those previously calculated for our face-sharing bioctahedral methoxycarbyne complexes,¹ or that derived from the semiempirical MO calculations carried out on the cluster $[\text{Co}_3(\mu_3\text{-COMe})(\text{CO})_9]$.²¹ This decrease in electron density at the carbyne atom of the methoxycarbyne ligand (when compared to the carboxycarbyne ligand) cannot be attributed to the presence of the already mentioned $\pi_{\text{C-O}}$ interaction in the former, since such an interaction is expected to increase (rather than decrease) the electron density at the C(carbyne) atom. Therefore the low negative charge at the bridgehead carbon atom of the methoxycarbyne ligand must be attributed essentially to the high electronegativity of the oxygen atom bound to it.

Optimized Geometries of the Tricarbonyl Complex 2. The optimized geometries of the tricarbonyl isomers *cis-2* and *trans-2* are fully consistent with the decrease in the intermetallic bond order and the high asymmetry expected for these molecules. The intermetallic distances found for both isomers (ca. 3.16 Å) are consistent with the electron-precise nature of these 34-electron complexes, for which a single metal–metal bond has to be proposed according to the EAN formalism, and they are significantly longer (by ca. 0.4 Å) than the corresponding lengths in the dicarbonyls **3** or **4**, as expected. In both isomers the metal atoms and the bridging phosphorus and carbon atoms define a puckered Mo_2CP rhombus, with dihedral angles of ca. 160° (*cis-2*) and 150° (*trans-2*). The most relevant feature in these central frameworks is the highly asymmetric coordination of the methoxycarbyne ligand in both cases, which is placed much closer to the monocarbonylic metal center. This asymmetry is so pronounced that the longer distance (ca. 2.35 Å) is remarkably greater than the value expected for a comparable Mo-C single bond, i.e., the distances found for symmetrically bridging carbonyl ligands (ca. 2.10 Å).^{1,5} Conversely, the second Mo-C bond length is much shorter, with a value of only 1.90 Å, a figure approaching that for the terminal methoxycarbyne complex ($[\text{WTP}'(\text{COMe})(\text{CO})_2]$; $\text{Tp}' = \text{HB}(\text{N}_2\text{C}_3\text{Me}_2\text{H})_3$; $\text{W} \equiv \text{C} = 1.86(1)$ Å).¹⁰ Thus we can describe the coordination of the methoxycarbyne ligand in these molecules as semibridging or nearly terminal, with an Mo-C bond close to triple (Chart 1), in agreement with the ^{13}C NMR data of compound **2** discussed above. The dicyclohexylphosphide bridge is also more strongly bound to the monocarbonylic metal fragment, but the asymmetry here is less pronounced, with the Mo-P lengths differing by ca. 0.2 Å.

A frequency analysis for both isomers (*cis-2* and *trans-2*) ensured that the optimized geometries correspond to real minima of the PES, and also allowed us to distinguish between both isomers on the basis of their IR patterns (Figure 2 and Table 3). The calculated patterns of the C–O stretching bands for both isomers are different enough to safely exclude the presence of significant amounts of the *trans*-isomer in the solutions of compound **2**, which exhibit an IR spectrum with the pattern calculated for the *cisoid* structure, and NMR resonances indicative of the presence of a single species in solution. Furthermore, we note that the *cisoid* structure is calculated to be slightly more stable than that of the isomer *trans-2* (by $\Delta G = 2$ kJ mol⁻¹ at 298 K and 1 atm). This small difference itself would not justify the absence of *trans-2* in solution, which possibly is less favored by the solute–solvent interactions, although we have not studied this effect.

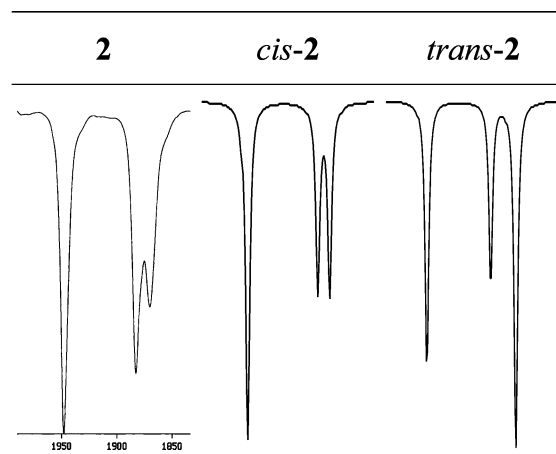


Figure 2. Experimental (left, petroleum ether solution) and DFT-calculated (middle and right) IR spectra for compound **2** in the C–O stretching region.

Molecular Orbitals of the 32-Electron Complexes 3 and 4. A detailed study of the molecular orbital diagrams for edge-sharing bioctahedral complexes was reported early by Hoffmann and co-workers,²² and was revisited and widened recently by some of us.²³ The metal–metal bonding in these systems follows from the occupation of one σ , one π , and one δ bonding MO's, with their corresponding antibonding combinations being the next ones in energy. Using this scheme as a first approach, we might therefore expect a configuration of the type $\sigma^2\pi^2\delta^2(\delta^*)^2$ for the 32-electron complexes **3** and **4**, and thus a formally double metal–metal bond, in agreement with the EAN formalism. This situation, however, could be significantly modified in our complexes as a result of orbital mixing with the π -acceptor ligands present there, as turns out to be the case.

The most relevant molecular orbitals of compounds **3** and **4** are depicted in Figure 3, along with their associated energy and prevalent bonding character. The occupied frontier orbitals exhibit some differences. In both compounds the highest occupied molecular orbital (HOMO) corresponds to the metal–metal δ^* orbital, with an important contribution of the $\pi^*_{\text{C-O}}$ orbitals of the terminal carbonyls, thus implying the presence of significant metal to carbon π back-bonding, which necessarily decreases the antibonding character of this orbital with respect to the metal–metal binding. Below this, there is a group of three orbitals with similar energies and then the corresponding δ -component of the Mo-Mo bond for these compounds [MO 120 (**3**) and MO 127 (**4**)]. The latter orbitals are so low in energy because of their pronounced delocalization over the Mo_2C triangle (by mixing with the relevant p orbital of the C atom), and hence represent effectively the π component of the metal–carbyne bond. A similar effect was previously found for our face-sharing bioctahedral methoxycarbyne complexes, in which one of the δ components of the triple metal–metal bond is involved in the π Mo-C bonding of the carbyne ligand.¹ The three orbitals below the HOMO in compounds **3** and **4** correspond to the σ and π components of the double metal–metal bond and to the upper-energy component of the metal–ligand σ -bonding orbitals holding the central Mo_2PC framework, but there are some differences in the metal–metal overlaps implied. For the carboxycarbyne complex **4**, the intermetallic

(22) Shaik, S.; Hoffmann, R.; Fiesel, C. R.; Summerville, R. H. *J. Am. Chem. Soc.* **1980**, *102*, 4555.

(23) Palacios, A. A.; Aullón, G.; Alemany, P.; Alvarez, S. *Inorg. Chem.* **2000**, *39*, 3166.

(21) Aitchison, A.; Farrugia, L. J. *Organometallics* **1987**, *6*, 819.

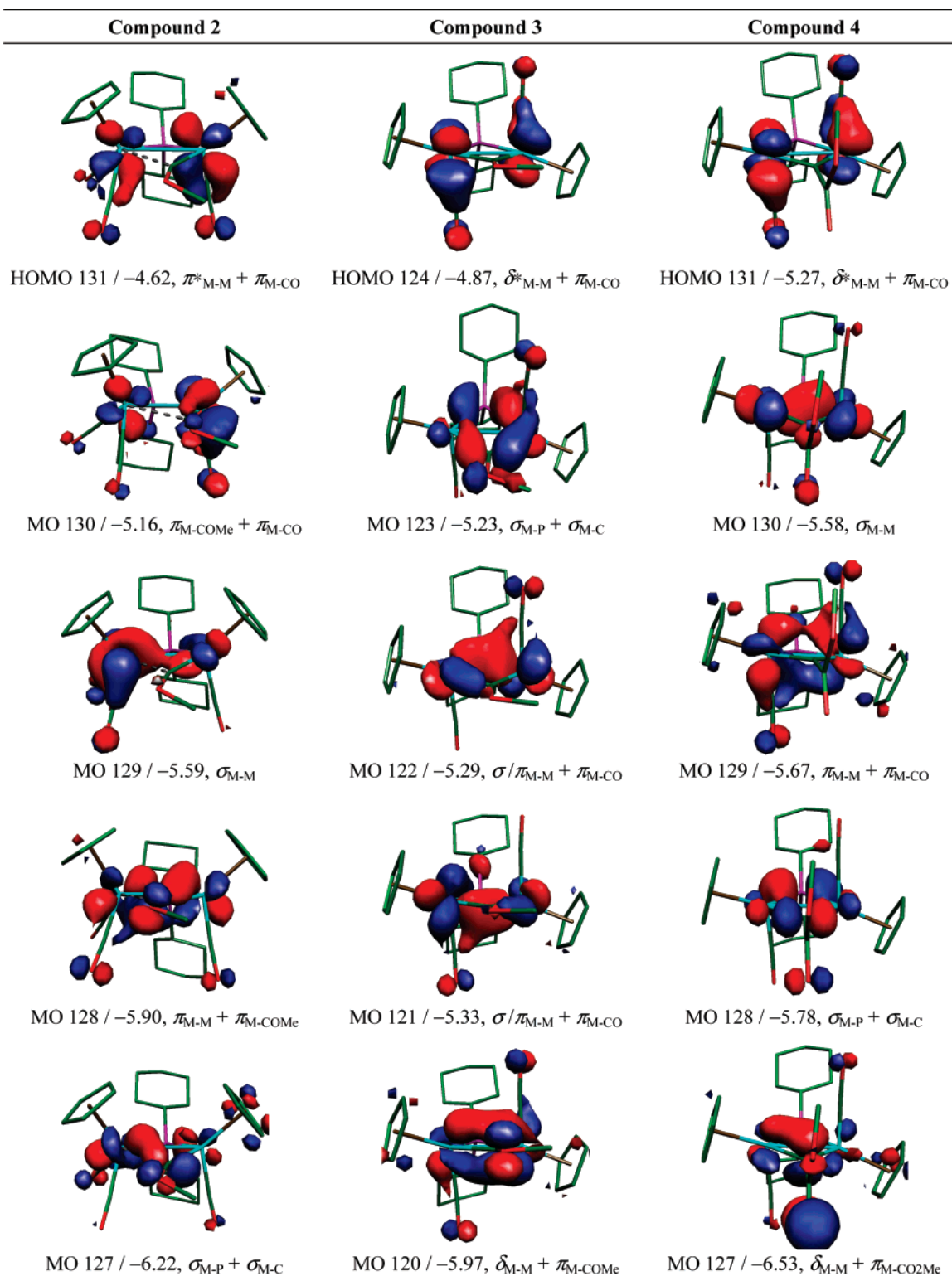


Figure 3. Selected molecular orbitals of complexes **2**, **3**, and **4**, with their energies and main bonding character indicated below.

bond consists of the two classical σ and π components, while for the methoxycarbonyl complex this bond is made up of two nearly equivalent bent (or banana) bonds. At the moment we can give no satisfactory explanation to this result.

As for the bonding within the methoxycarbonyl moiety, there is a molecular orbital (MO 103, see Table S3 in the Supporting Information) that reveals the presence of significant π -bonding interaction in the O-C(carbyne) bond of this ligand, therefore competing with the Mo-C π bonding (MO 120), as found for our 30-electron methoxycarbonyl complexes,¹ and thus this needs

not be further discussed. Finally we note that the lowest unoccupied molecular orbitals (LUMO) of these dicarbonyl complexes are largely metal-based molecular orbitals (MO 125 (**3**) and MO 132 (**4**), see the Supporting Information), and exhibit π^*_{M-M} antibonding character. As could be expected for such unsaturated molecules, the incorporation of electron-donor ligands to the dinuclear center under orbital-controlled conditions is to be accompanied by a reduction of the intermetallic bond order. In fact, for the complex **2**, which is the CO-addition

Table 4. Topological Properties of the Electron Density at the Bond Critical Points^a

bond	2		3		4	
	ρ	$\nabla^2\rho$	ρ	$\nabla^2\rho$	ρ	$\nabla^2\rho$
Mo1–Mo2			0.419 ^b	1.66 ^b	0.444 ^b	1.98 ^b
Mo1–C*	0.478	3.23	0.918	6.23	0.918	6.65
Mo1–C*			0.929 ^b	5.29 ^b	0.925 ^b	5.81 ^b
Mo2–C*	1.085	8.30	0.866	6.73	0.938	6.96
Mo2–C*			0.874 ^b	5.89 ^b	0.902 ^b	6.14 ^b
C*–OMe	2.084	0.82	2.029	2.47		
O–Me	1.582	−9.95	1.633	−11.08	1.651	−9.97
	0.885	10.68				
Mo1–CO	0.865	10.08	0.885	10.20	0.862	10.09
Mo2–CO	0.901	11.27	0.878	10.24	0.877	9.87
C–O	2.984	24.75	2.956	23.51	2.990	25.02
	2.975	24.22	2.952	23.40	2.969	24.10
	2.938	22.70				
Mo1–P	0.499	2.14	0.528	3.27	0.526	3.17
Mo2–P	0.560	3.22	0.523	3.00	0.524	3.12
C*–CO ₂ Me					1.927	−18.29
C=O(OMe)					2.736	3.97
C(O)–OMe					1.956	−11.52
C*MoPMo ^c	0.203	1.150	0.362	1.62	0.374	1.62
MoC*Mo ^c			0.419 ^b	2.03 ^b	0.444 ^b	2.13 ^b

^a Values of the electron density at the bond critical points (ρ) are given in $e \text{ \AA}^{-3}$; values of the laplacian of ρ at these points ($\nabla^2\rho$) are given in $e \text{ \AA}^{-5}$; Mo1 refers to the atom positioned trans to the methyl group of the COME ligand, except for compound **4**, for which the labeling is arbitrary; C* refers to the bridgehead atom of the carbyne ligand; all the data were computed with the LANL2DZ ECP. ^b Data computed with the SDD ECP. ^c Values at the ring critical point.

product of **3**, we find a longer metal–metal distance, in agreement with this bond-order reduction, as discussed below.

Molecular Orbitals of cis-2. The MO's of this highly asymmetric molecule exhibit a strong mixing of atomic orbitals and are difficult to interpret. The HOMO of this compound is a π^* combination of metal AO's with a significant contribution of the π^*_{C-O} orbital of the terminal carbonyls, and correlates in shape with the LUMO of its precursor **3**, as expected. Mixing with the π^*_{C-O} orbital of the terminal carbonyls is also observed in the orbitals following the HOMO, which represent the Mo–Mo σ bond (MO 129) and the Mo–C(carbyne) π bonding. In contrast to the tricentric π bonding interaction between both metal centers and the C(carbyne) atom that is found for the symmetrically bridged carbyne complexes **3** or **4**, the corresponding π interaction in **2** is now more localized between the carbon atom and the monocarbonyl metal center, and it can be recognized through the orbitals MO 130 (Mo–C π bonding) and MO 128 (distorted tricentric Mo–C–Mo π bonding). This is in agreement with the geometric parameters already discussed, revealing a very asymmetric binding of the carbyne ligand, strongly bound to the monocarbonylic center.

Topological Analysis of the Electron Density. In the previous part of this series we have shown that the analysis of the electron density under the AIM theory provides very valuable information (complementary to that of the MO analysis) for the characterization, interpretation and even quantification of the different bonds present in our highly unsaturated 30-electron methoxycarbyne complexes.¹ We have therefore performed a similar analysis for the complexes **2** to **4**, with special attention to the data relative to the metal–metal and metal–carbyne bonds. The values of the electron density (ρ) and its laplacian ($\nabla^2\rho$) at the most relevant bond critical points (bcp) of these complexes are collected in Table 4.

The first significant observation is that in none of the cases could a Mo–Mo bcp be located with the usual basis set (Figure 4), a circumstance previously found for other carbonyl com-

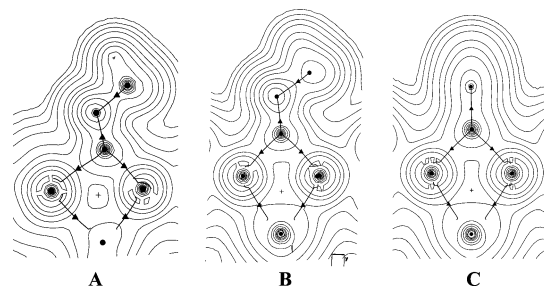


Figure 4. Electron density maps in the Mo₂C(carbyne) plane of compounds **2** (A), **3** (B), and **4** (C). Nuclear positions (●), bond critical points (▲), ring critical points (+), and bond critical paths (bold lines) are also indicated.

plexes with chemically predictable M–M bonds,²⁴ such as [Co₂(CO)₈]²⁵ and [Fe₂(CO)₉],²⁶ or for the phosphide-bridged complexes [Fe₂(μ -H)_x(μ -PH₂)(CO)₄(PH₃)₂]^{(x-1)+} ($x = 1, 2$).²⁷ Since the quality of the DFT-derived electron density is quite dependent on the basis sets used, we then tested different combinations of basis sets and effective core potentials (ECP). The best results were obtained when using a combination of the Stuttgart–Dresden relativistic effective core potentials (SDD-RECP) for molybdenum atoms and 6-31G* basis for light atoms. These computations were carried out on the previously optimized structures for these complexes, since we did not observe significant differences between the optimized structure of the complex **3** by using either the LANL2DZ or the SDD pseudopotentials. Keeping in mind the relativistic derivation of the SDD ECP, we can assume that it will yield a more accurate description of the electron density especially in the intermetallic region, then being more reliable to analyze the metal–metal bonding. The values of ρ and its laplacian so computed at the Mo–Mo and Mo–C(carbyne) bcp's for compounds **3** and **4** have been added to Table 4 (the values for other bonds were similar to those obtained with the usual basis set and are not included).

First, we note that the use of the SDD/6-31G* basis for the dicarbonyl complexes **3** and **4** leads to the location of the corresponding metal–metal bcp's (Figure 5). As expected, the values of ρ at these points (ca. 0.43 $e \text{ \AA}^{-3}$) are intermediate between those calculated for triply bonded carbonyl complexes (ca. 0.60 $e \text{ \AA}^{-3}$) and that computed for the singly bonded [Mo₂Cp₂(CO)₆] (ca. 0.17 $e \text{ \AA}^{-3}$),¹ which is in agreement with the double metal–metal bond proposed for these 32-electron complexes, also sustained by the MO analysis. In contrast, no intermetallic bcp could be located for the tricarbonyl **2**, probably due to the much longer M–M separation, this leading to a quite flat plateau of almost equal ρ along the intermetallic vector (Figure 5), where the mathematical conditions of the bcp cannot be satisfied. Note, however, that the electron density at the intermetallic region of **2** does not vanish, but keeps a minimum value of ca. 0.22 $e \text{ \AA}^{-3}$, similar to the density of the singly bonded [Mo₂Cp₂(CO)₆] at the intermetallic bcp (ca. 0.17 $e \text{ \AA}^{-3}$).¹ Finally, we note that the values of $\nabla^2\rho$ at the intermetallic bcp for compounds **3** and **4** are moderately positive (1.65–2.76 $e \text{ \AA}^{-5}$). This feature was also found for our 30-electron methoxycarbyne complexes,¹ and seems to be a characteristic of

(24) Macchi, P.; Sironi, A. *Coord. Chem. Rev.* **2003**, 238–239, 383.

(25) Low, A. A.; Kunze, K. L.; MacDougall, P. J.; Hall, M. B. *Inorg. Chem.* **1991**, 30, 1079.

(26) Bo, C.; Sarasa, J. P.; Poblet, J. M. *J. Phys. Chem.* **1993**, 97, 6362.

(27) Phillips, A.; Ienco, A.; Reinhold, J.; Böttcher, H.-C.; Mealli, C. *Chem. Eur. J.* **2006**, 12, 4691.

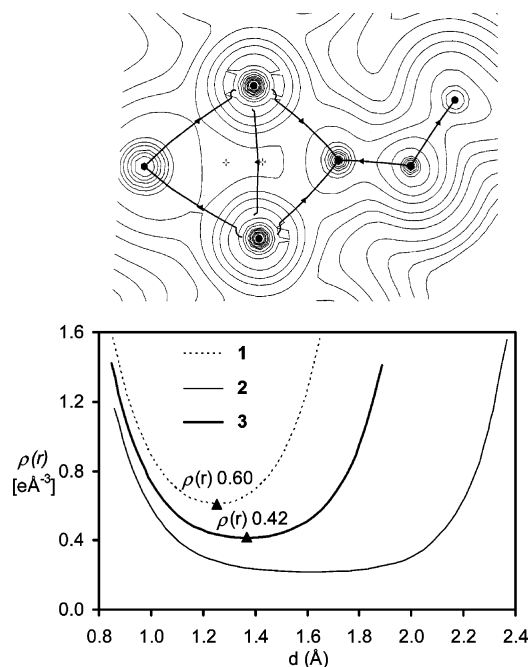


Figure 5. Electron density map in the $\text{Mo}_2\text{C}(\text{carbyne})$ plane of complex **3**, with nuclear positions (●), bond critical points (▲), ring critical points (+), and bond critical paths (bold lines) also indicated (top). Below are represented the electron density profiles along the metal–metal vector for the complexes **1**, **2**, and **3**.

metal–metal interactions in transition metal complexes,²⁸ attributed to the diffuse character of the electrons involved in the bonding.²⁴

As for the M–C(carbyne) bonds, the values of ρ at the corresponding bcp's in the dicarbonyls **3** and **4** are quite similar, with figures close to the values calculated for our 30-electron methoxycarbyne complexes (in the range $0.83\text{--}0.93\text{ e \AA}^{-3}$).¹ The average value for the carboxycarbyne complex **4** (0.93 e \AA^{-3}) is only slightly higher than the corresponding average value for the methoxycarbyne complex **3** (0.90 e \AA^{-3}). From these data we can conclude that the strength of the interaction between the dimetal center and a COR ligand is not significantly different from that of a CR ligand having an electron-withdrawing hydrocarbon group. The tricarbonyl **2** displays a strongly asymmetric coordination of the carbyne ligand, and this causes the electron density at the bcp of the shorter bond to be considerably higher (1.09 e \AA^{-3}) than the values calculated for symmetrical methoxycarbyne bridges,¹ indeed approaching the electron density calculated for the terminal carbyne $\text{Cr}\equiv\text{CH}$ (1.17 e \AA^{-3}).²⁹ Conversely, the longer Mo–C bond in *cis*-**2** is characterized by a much lower value of ρ at the corresponding bcp (0.48 e \AA^{-3}), which is substantially lower than the values found for comparable M–C single bonds, such as the electron density calculated for CrCH_3 (0.77 e \AA^{-3}),²⁹ or the values of ca. 0.71 e \AA^{-3} found for the Mo–C bonds of the carbonyl bridges in our 30-electron complexes.¹ This justifies our description of the coordination of the carbyne ligand in **2** as strongly semibridging, with Mo–C bonds of orders higher than two and lower than one, respectively (Chart 1).

The bonding within the CO_2Me substituent of the carbyne ligand of **4** is comparable to that of this fragment in an organic

ester like the methyl acetate, as far as the values of ρ and its laplacian are concerned (see Table 4 and the Supporting Information), except for the value of ρ at the bcp of the C– $\text{CO}_2\text{-Me}$ bond in **4** (1.93 e \AA^{-3}), somewhat higher than the corresponding figure for the Me–C bond in methyl acetate (1.75 e \AA^{-3}), as expected when comparing $\text{C}(\text{sp}^2)\text{--C}(\text{sp}^2)$ and $\text{C}(\text{sp}^3)\text{--C}(\text{sp}^2)$ bonds (shorter interatomic separation in the former bonds). It is important to notice that all these bonds exhibit large negative values of $\nabla^2\rho$, in agreement with their covalent nature.¹⁴ From this general behavior, however, we have to exclude the C=O bond, which exhibits a positive value for this function at the corresponding bcp (3.97 and 4.45 e \AA^{-5} for **4** and methyl acetate, respectively). Actually this is the usual feature found for multiple C–O bonds, and can be mainly attributed to the displacement of the bcp toward the carbon atom.²⁴

As for the C–OMe bonds in the methoxycarbyne complexes *cis*-**2** and **3** we find that the electron density at the corresponding bcp's (ca. 2.05 e \AA^{-3}) has values comparable to those found for our 30-electron methoxycarbyne complexes ($2.03\text{--}2.13\text{ e \AA}^{-3}$),¹ and all these are in turn slightly higher than the values found for the C(O)–OMe bonds in **4** or methyl acetate. We take this alone as an indication of the presence of some multiplicity in the C–OMe bonds of our methoxycarbyne complexes. Besides this, there is an independent feature pointing to the same conclusion: the values for the laplacian of ρ at the C–OMe bcp's in all our methoxycarbyne complexes are positive (ca. $0.8\text{--}2.5\text{ e \AA}^{-5}$, see Table 4 and ref 1), a common feature of multiple C–O bonds as stated above, while the corresponding figures for the C(O)–OMe bonds in **4** or methyl acetate keep the high negative values (ca. -11.5 e \AA^{-5}) expected for single covalent C–O bonds.

Concluding Remarks

The 30-electron methoxycarbyne complex **1** does behave as a substrate having a triple intermetallic bond, then being able to incorporate two CO molecules to give the corresponding electron-precise tricarbonyl complex **2**, which in turn renders the 32-electron tricarbonyl **3** through a reversible thermal decarbonylation. The DFT methods used to study these complexes lead to optimized geometries which in the case of its unsaturated dicarbonyl **3** are in excellent agreement with that experimentally determined for the related carboxycarbyne complex **4**, and the frequency calculation for the two possible isomers of the tricarbonyl **2** allows the unambiguous identification of its dominant structure in solution as the *cisoid* one. The analysis of the molecular orbitals for the 32-electron edge-sharing bioctahedral complexes **3** and **4** gives support to the presence of a double metal–metal bond derived from a configuration of the type $\delta^2\sigma^2\pi^2(\delta^*)$,² in which the δ^* orbitals are involved in the π back-bonding to the terminal carbonyls, while the δ orbitals are delocalized over the $\text{Mo}_2\text{C}(\text{carbyne})$ triangle and then constitute the π -bonding component of the metal–carbyne bond, which is very similar in both the methoxycarbyne and the carboxycarbyne ligands. Yet, some residual π -bonding interaction at the C–O bond of the methoxycarbyne ligand can be identified, which weakens the Mo–C bond of this ligand to a small extent. The tricarbonyl **2** exhibits a methoxycarbyne ligand with a strongly asymmetric, nearly terminal coordination to the metal atoms, with the latter kept at a short distance by a σ -type bonding orbital.

The topological analysis of the electron density within all these molecules is fully consistent with the MO description of the bonding just given. In particular, we find that the electron

(28) Gervasio, G.; Bianchi, R.; Marabello, D. *Chem. Phys. Lett.* **2004**, 387, 481 and references cited therein.

(29) Vidal, I.; Melchor, S.; Dobado, J. A. *J. Phys. Chem.* **2005**, 109, 7500.

density in the intermetallic region of these molecules reaches a relatively flat plateau. As a result, only for the double-bonded dicarbonyls **3** and **4**, and using a high quality basis, can the intermetallic bcp's be located, with values of ρ at these points of ca. $0.4 \text{ e } \text{\AA}^{-3}$, which are figures intermediate between those of the triply bonded $[\text{Mo}_2\text{Cp}_2(\text{CO})_4]$ and the singly bonded $[\text{Mo}_2\text{Cp}_2(\text{CO})_6]$. The electron densities at the Mo–C bonds of the dicarbonyl complexes **3** and **4** are similar, and then support the idea that the strengths of binding to the metal of the methoxy-carbyne and carboxycarbyne ligands are comparable, with the former being slightly weakened because of the presence of some π -interaction in the C–OMe bond, which in turn is supported by the relatively high value of ρ and positive (instead of negative) value of its laplacian at the corresponding bond critical point.

Experimental Section

General Procedures and Starting Materials. All manipulations and reactions were carried out under a nitrogen (99.995%) atmosphere with standard Schlenk techniques. Solvents were purified according to literature procedures and distilled prior to use.³⁰ Petroleum ether refers to that fraction distilling in the range 338–343 K. Compound **1** was prepared as described previously.⁵ Chromatographic separations were carried out with use of jacketed columns cooled by a closed 2-propanol circuit, kept at the desired temperature with a cryostat. Commercial aluminum oxide (Aldrich, activity I, 150 mesh) was degassed under vacuum prior to use. The latter was mixed under nitrogen with the appropriate amount of water to reach the activity desired. All other reagents were obtained from the usual commercial suppliers and used as received. IR stretching frequencies were measured in solution and are referred to as ν (solvent). Nuclear magnetic resonance (NMR) spectra were routinely recorded at 300.13 (¹H), 121.50 (³¹P{¹H}), or 75.47 (¹³C-{¹H}) at 290 K in CD₂Cl₂ solutions unless otherwise stated. Chemical shifts (δ) are given in ppm, relative to internal tetramethylsilane (¹H, ¹³C) or external 85% aqueous H₃PO₄ (³¹P). Coupling constants (J) are given in Hz.

Preparation of $[\text{Mo}_2\text{Cp}_2(\mu\text{-COMe})(\mu\text{-PCy}_2)(\text{CO})_3]$ (2**).** A toluene solution (10 mL) of compound **1** (0.100 g, 0.169 mmol) was placed in a bulb equipped with a Young's valve. The bulb was cooled at 77 K, evacuated under vacuum, and then refilled with CO. The valve was then closed, and the solution was allowed to reach room temperature and further stirred for 14 h to give an orange solution containing compound **2** as the major product. After removal of solvents under vacuum, dichloromethane (10 mL) and then petroleum ether (15 mL) were added. Removal of the solvents from the latter mixture under vacuum gave compound **2** as an orange powder (0.099 g, 91%). Anal. Calcd for C₂₇H₃₅Mo₂O₄P: C, 50.17; H, 5.46. Found: C, 50.21; H, 5.39. ν_{CO} (CH₂Cl₂) 1933 (vs), 1860 (s), 1843 (m, sh) cm⁻¹. ¹H NMR δ 5.34, 5.00 (2 \times s, 2 \times 5H, 2 \times Cp), 4.44 (s, 3H, OMe), 2.5–0.4 (m, 22H, Cy). ³¹P-{¹H} NMR δ 219.7 (s). ¹³C{¹H} NMR δ 300.7 (d, $J_{\text{CP}} = 9$, $\mu\text{-COMe}$), 242.8 (d, $J_{\text{CP}} = 27$, CO), 238.3 (d, $J_{\text{CP}} = 10$, CO), 236.5 (s, CO), 92.9, 90.9 (2 \times s, 2 \times Cp), 70.5 (s, OMe), 54.8 [d, $J_{\text{CP}} = 12$, C¹(Cy)], 39.5 [d, $J_{\text{CP}} = 16$, C¹(Cy)], 36.0 [d, $J_{\text{CP}} = 3$, C^{2,6}(Cy)], 35.1 [s, C^{2,6}(Cy)], 34.6 [d, $J_{\text{CP}} = 3$, C^{2,6}(Cy)], 29.2 [s, C^{2,6}(Cy)], 28.9 [d, $J_{\text{CP}} = 9$, C^{3,5}(Cy)], 28.6 [d, $J_{\text{CP}} = 10$, C^{3,5}(Cy)], 27.9 [d, $J_{\text{CP}} = 13$, C^{3,5}(Cy)], 27.7 [d, $J_{\text{CP}} = 14$, C^{3,5}(Cy)], 26.8 [s, C⁴(Cy)], 26.5 [s, C⁴(Cy)].

Preparation of $[\text{Mo}_2\text{Cp}_2(\mu\text{-COMe})(\mu\text{-PCy}_2)(\text{CO})_2]$ (3**).** A toluene solution (20 mL) of compound **2** (0.080 g, 0.124 mmol) was stirred at 333 K for 45 min to give a red solution containing compound **3** as the major product. Solvents were then removed

under vacuum and the residue was dissolved in dichloromethane–petroleum ether (1:4) and chromatographed on an alumina column (activity IV, 20 \times 2 cm) at 253 K. Elution with dichloromethane–petroleum ether (1:2) gave a pale pink fraction that yielded, after removal of solvents, compound **3** as a red microcrystalline solid (0.52 g, 68%). Anal. Calcd for C₂₆H₃₅Mo₂O₃P: C, 50.50; H, 5.70. Found: C, 50.67; H, 5.93. ν_{CO} (CH₂Cl₂) 1894 (w, sh), 1863 (s) cm⁻¹. ¹H NMR δ 5.45 (s, 10H, Cp), 4.78 (s, 3H, OMe), 2.4–1.1 (m, 22H, Cy). ³¹P{¹H} NMR δ 125.0 (s). ¹³C{¹H} NMR δ 404.0 (d, $J_{\text{CP}} = 5$, $\mu\text{-COR}$), 227.8 (d, $J_{\text{CP}} = 11$, CO), 90.2 (s, Cp), 70.5 (s, OMe), 44.9 [d, $J_{\text{CP}} = 19$, C¹(Cy)], 36.0 [s, C^{2,6}(Cy)], 34.2 [s, C^{2,6}(Cy)], 28.5 [d, $J_{\text{CP}} = 8$, C^{3,5}(Cy)], 28.4 [d, $J_{\text{CP}} = 10$, C^{3,5}(Cy)], 26.6 [s, C⁴(Cy)].

Computational Details. All computations described in this work were carried out with the GAUSSIAN03 package,³¹ in which the hybrid method B3LYP was applied with the Becke three parameters exchange functional³² and the Lee–Yang–Parr correlation functional.³³ Effective core potentials (ECP) and their associated double- ζ LANL2DZ basis set were used for the molybdenum and phosphorus atoms,³⁴ supplemented by an extra d-polarization function in the case of P.³⁵ The light elements (O, C, and H) were described with 6-31G* basis.³⁶ Geometry optimizations were performed under no symmetry restrictions, using initial coordinates derived from X-ray data of the same or comparable complexes, and frequency analyses were performed to ensure that a minimum structure with no imaginary frequencies was achieved in each case. For interpretation purposes, natural population analysis (NPA) charges^{19b} were derived from the natural bond order (NBO) analysis of the data.^{19b} Molecular orbitals and vibrational modes were visualized by using the Molekel program.³⁷ For the AIM analysis of ρ we also carried out single-point calculations on the previously optimized geometries but using a combination of the relativistic effective core potentials (RECP) from the Stuttgart–Dresden group (SDD) to represent the innermost electrons of the Mo atom together with their associated valence basis set of double- ζ quality,³⁸ and the 6-31G* basis for light elements. The topological analysis of ρ was carried out with the *Xaim* routine.³⁹

(31) Frisch, M. J.; Trucks, G. W.; Schlegel, H. B.; Scuseria, G. E.; Robb, M. A.; Cheeseman, J. R.; Montgomery, J. A., Jr.; Vreven, T.; Kudin, K. N.; Burant, J. C.; Millam, J. M.; Iyengar, S. S.; Tomasi, J.; Barone, V.; Mennucci, B.; Cossi, M.; Scalmani, G.; Rega, N.; Petersson, G. A.; Nakatsuji, H.; Hada, M.; Ehara, M.; Toyota, K.; Fukuda, R.; Hasegawa, J.; Ishida, M.; Nakajima, T.; Honda, Y.; Kitao, O.; Nakai, H.; Klene, M.; Li, X.; Knox, J. E.; Hratchian, H. P.; Cross, J. B.; Bakken, V.; Adamo, C.; Jaramillo, J.; Gomperts, R.; Stratmann, R. E.; Yazyev, O.; Austin, A. J.; Cammi, R.; Pomelli, C.; Ochterski, J. W.; Ayala, P. Y.; Morokuma, K.; Voth, G. A.; Salvador, P.; Dannenberg, J. J.; Zakrzewski, V. G.; Dapprich, S.; Daniels, A. D.; Strain, M. C.; Farkas, O.; Malick, D. K.; Rabuck, A. D.; Raghavachari, K.; Foresman, J. B.; Ortiz, J. V.; Cui, Q.; Baboul, A. G.; Clifford, S.; Cioslowski, J.; Stefanov, B. B.; Liu, G.; Liashenko, A.; Piskorz, P.; Komaromi, I.; Martin, R. L.; Fox, D. J.; Keith, T.; Al-Laham, M. A.; Peng, C. Y.; Nanayakkara, A.; Challacombe, M.; Gill, P. M. W.; Johnson, B.; Chen, W.; Wong, M. W.; Gonzalez, C.; Pople, J. A. *Gaussian 03*, Revision B.02; Gaussian, Inc.: Wallingford, CT, 2004.

(32) Becke, A. D. *J. Chem. Phys.* **1993**, *98*, 5648.

(33) Lee, C.; Yang, W.; Parr, R. G. *Phys. Rev. B* **1988**, *37*, 785.

(34) Hay, P. J.; Wadt, W. R. *J. Chem. Phys.* **1985**, *82*, 299.

(35) Höllwarth, A.; Böhme, M.; Dapprich, S.; Ehlers, A. W.; Gobbi, A.; Jonas, V.; Köhler, K. F.; Stegman, R.; Veldkamp, A.; Frenking, G. *Chem. Phys. Lett.* **1993**, *208*, 237.

(36) (a) Hariharan, P. C.; Pople, J. A. *Theor. Chim. Acta* **1973**, *28*, 213. (b) Petersson, G. A.; Al-Laham, M. A. *J. Chem. Phys.* **1991**, *94*, 6081. (c) Petersson, G. A.; Bennett, A.; Tensfeldt, T. G.; Al-Laham, M. A.; Shirley, W. A.; Mantzaris, J. *J. Chem. Phys.* **1988**, *89*, 2193.

(37) Portmann, S.; Lüthi, H. P. MOLEKEL: An Interactive Molecular Graphics Tool. *CHIMIA* **2000**, *54*, 766.

(38) Andrae, D.; Haussermann, U.; Dolg, M.; Stoll, H.; Preuss, H. *Theor. Chim. Acta* **1990**, *77*, 123.

(39) Ortiz, J. C.; Bo, C. *Xaim*; Departamento de Química Física e Inorgánica, Universidad Rovira i Virgili: Tarragona, Spain, 1998.

(30) Amarego, W. L. F.; Chai, C. *Purification of Laboratory Chemicals*, 5th ed.; Butterworth-Heinemann: Oxford, UK, 2003.

Acknowledgment. We thank the MEC of Spain for a grant (to D.G.) and financial support (Projects BQU2003-05471 and CTQ2005-08123-C02-02BQU). The computing resources at the Centre de Supercomputació de Catalunya (CESCA) were made available to us through a grant from Fundació Catalana per a la Recerca (FCR) and Universitat de Barcelona.

Supporting Information Available: Mulliken and NPA charges, molecular orbitals, and data from the AIM topological analysis for complexes **2**, **3**, and **4**. This material is available free of charge via the Internet at <http://pubs.acs.org>.

OM700735G